



## **Prediction of Differential Track Settlement in Transition Zones Using a Non-Linear Track Model**

Downloaded from: <https://research.chalmers.se>, 2026-06-11 22:13 UTC







Citation for the original published paper (version of record):

Nasrollahi, K., Nielsen, J., Aggestam, E. et al (2022). Prediction of Differential Track Settlement in Transition Zones Using a Non-Linear Track Model. Lecture Notes in Mechanical Engineering: 282-292. [http://dx.doi.org/10.1007/978-3-031-07305-2\\_29](http://dx.doi.org/10.1007/978-3-031-07305-2_29)

N.B. When citing this work, cite the original published paper.



# Prediction of Differential Track Settlement in Transition Zones Using a Non-Linear Track Model

Kourosh Nasrollahi<sup>1</sup>  , Jens C. O. Nielsen<sup>1</sup> , Emil Aggestam<sup>1</sup> ,  
Jelke Dijkstra<sup>2</sup> , and Magnus Ekh<sup>3</sup> 

- <sup>1</sup> Department of Mechanics and Maritime Sciences, Chalmers University of Technology,  
412 96 Gothenburg, Sweden  
Kourosh@chalmers.se
- <sup>2</sup> Department of Architecture and Civil Engineering, Chalmers University of Technology,  
412 96 Gothenburg, Sweden
- <sup>3</sup> Department of Industrial and Materials Science, Chalmers University of Technology,  
412 96 Gothenburg, Sweden

**Abstract.** An iterative simulation procedure for the prediction of differential settlement of ballast/subgrade in a transition zone between two track forms is presented. The procedure is based on a time-domain model of vertical dynamic vehicle–track interaction to calculate the contact loads between sleepers and ballast in the short-term, which are then used in an empirical model to determine the settlement of ballast/subgrade below each sleeper in the long-term. The procedure is applied for a transition zone between a 3MB slab track and a ballasted track. Each sleeper in the ballasted track section is modelled by a discrete (rigid) mass. Non-linear sleeper support conditions and the possible development of hanging sleepers over time due to settlement are considered. For heavy-haul traffic, the influence of axle load and train speed on the long-term settlement at the transition is studied in a demonstration example.

**Keywords:** Transition zone · Settlement model · Dynamic vehicle–track interaction · Non-linear track model · Simulation · Heavy-haul traffic

## 1 Introduction

In transition zones between two different track forms, there is a discontinuity in track structure leading to a gradient in track stiffness [1]. Examples include transitions between different superstructures, e.g., slab track to ballasted track, and/or between different substructures, e.g., embankment to a bridge or tunnel structure. Further, differences in loading and support conditions at the interfaces between track superstructure and substructure on either side of the transition may lead to differential track settlement and an irregularity in longitudinal rail level soon after construction. This results in an amplification of the dynamic traffic loading along the transition, contributing to the degradation process of ballast and subgrade and resulting in a further deterioration of

vertical track geometry. Hence, track adjacent to a transition is prone to deteriorate at an accelerating rate, and frequent maintenance work may be required [1].

Even though ballasted track is the most common track form, the use of slab track on high-speed lines has increased [2]. Compared to ballasted track, slab track has several advantages, e.g. higher lateral track resistance and eliminated problem with ballast degradation. These advantages reduce the need for maintenance and extend service life. However, when maintenance work on slab track is required, it is often more expensive compared to maintenance work on ballasted track. Over the years, slab track technology has been improved and optimized, and by considering prefabricated slab track systems the initial cost ratio compared to ballasted track has been reduced. For example, the “Moulded Modular Multi-Blocks slab-track” (3MB) concept is a reinforced standard precast slab designed for both mixed traffic and high-speed traffic. The slab panels can be set up both on bituminous and concrete subgrade layers [3].

However, as more slab track is built, more transitions between different track forms may be introduced. To reduce the required maintenance work associated with transitions, various types of transition zones can be installed. Different approaches of transition zone design have been applied, where the key idea is to reduce the dynamic loads and differential settlement by making the softer track stiffer and the stiffer track softer adjacent to the transition [1].

To predict the degradation of vertical track geometry, it is common to combine a simulation model of dynamic vehicle–track interaction in the short-term with an empirical model of long-term settlement. A review of empirical track settlement models has been presented by Abadi et al. [4]. In several models, the settlement is calculated as a function of the logarithm of the number of load cycles. However, generally these models do not account for the variation and redistribution of loads supporting the adjacent sleepers, as well as the occurrence of hanging sleepers over time due to settlement.

In this paper, an iterative procedure for the prediction of differential track settlement in a transition zone between slab track and ballasted track is presented. The track model is a non-linear finite element model accounting for gravity load, state-dependent foundation stiffness and hanging sleepers, while the empirical settlement equation is based on similar ideas as for a visco-plastic material mechanics model. Further, to demonstrate the procedure for heavy-haul traffic, the influence of axle load and train speed on dynamic loads and long-term settlement in a transition between ballasted track and slab track is investigated. Note that, in the demonstration examples, the track irregularity has been limited to the irregularity due to the differential settlement at the transition.

## 2 Modelling and Simulation of Vertical Vehicle-Track Interaction

In this paper, a two-dimensional model for the simulation of vertical dynamic vehicle–track interaction in a transition zone between two different track forms is presented, see Fig. 1. In the demonstration example, the vehicle is moving from a softer track section (ballasted track) to a stiffer one (slab track based on a modular concept, see [3]).

Thus, the transition zone track model consists of two sections: the ballasted track and the 3MB slab track. Symmetric vehicle and track properties with reference to the centre line of the track, and a symmetric excitation due to the same vertical track irregularity on

both rails, are assumed. This means that only the wheels on one side of the wheelsets, one of the rails, half of the slab and half sleepers are included in the model. The foundation stiffness in the slab track section is modelled as linear and any evolution of differential settlement is neglected relative to the settlement in the ballasted track section. This is because the contact pressure between base slab and foundation is expected to be significantly lower than the corresponding contact pressure below each sleeper. In the ballasted track section, the state-dependent stiffness and damping of the ballast and foundation under each sleeper is modelled as a spring-damper connection with piecewise linear properties. This will allow for hanging sleepers that may develop due to the accumulated differential settlement of the foundation.

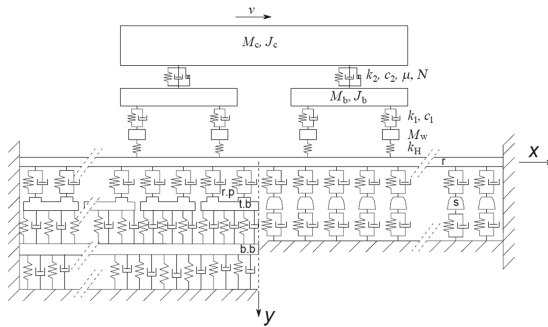


**Fig. 1.** Complete track and vehicle models. The track model consists of rail (r), top block (t.b) and base block (b.b) that are all modelled by Euler-Bernoulli beam elements. The bottom block is supported by a Winkler foundation. The sleepers (s) are rigid masses supported by a spring-damper connection (representing the ballast/subgrade) with piecewise linear stiffness properties

### 2.1 Railway Track Model

The non-linear track model is a finite element model with rigid boundaries at both rail ends and at the lower connection point of each spring/damper model representing the ballast and subgrade. In Fig. 1, the length of the track model is set to 54 m (corresponding to 36 m of ballasted track and 18 m of slab track). Each sleeper in the ballasted track section is modelled by one discrete (rigid) element with one vertical degree of freedom (DOF) and mass  $m_s = 150$  kg and positioned at uniform sleeper distance  $L_i = 0.6$  m, while the two-layer slab track is modelled by one continuous beam representing the base slab below a layer of discrete blocks. Rail properties are labelled with index ‘r’. The two layers of the 3MB slab track are labelled ‘t.b’ and ‘b.b’, respectively. Each layer of beam elements has bending stiffness  $EI_A(X)$ <sup>1</sup> and mass  $m_A(X)$  per unit beam length, width  $b_A$  and height  $h_A(X)$  that may vary along the longitudinal track coordinate. The connection between each pair of adjacent nodes in the different layers is modelled as a

<sup>1</sup> Replace A with the label of the considered layer (r, t.b or b.b).

spring and viscous damper in parallel and is denoted as  $B_{CD}$ <sup>2</sup>. Input data for the track model are provided in Tables 1 and 2.

**Table 1.** Beam properties in the track model

Rail	Top block	Bottom block
$EI_r = 6.4 \text{ MN m}^2$	$EI_{t,b} = 11 \text{ MN m}^2$	$EI_{b,b} = 23.45 \text{ MN m}^2$
$m_r = 60 \text{ kg/m}$	$m_{t,b} = 275 \text{ kg/m}$	$m_{b,b} = 375 \text{ kg/m}$
	$b_{t,b} = 0.55 \text{ m}$	$b_{b,b} = 0.6 \text{ m}$
	$h_{t,b} = 0.2 \text{ m}$	$h_{b,b} = 0.25 \text{ m}$

**Table 2.** Stiffness and viscous damping of resilient layers in the track model

Stiffness	Damping
$k_f = 100 \text{ MN/m}^3$	$c_f = 82 \text{ kNs/m}^3$
$k_{r/s} = 120 \text{ MN/m}$	$c_{r/s} = 25 \text{ kNs/m}$
$k_{r/t,b} = 40 \text{ MN/m}$	$c_{r/t,b} = 10 \text{ kNs/m}$
$k_{t,b/b,b} = 1.0 \text{ GN/m}^3$	$c_{t,b/b,b} = 250 \text{ kNs/m}$

## 2.2 Vehicle Model

The iron ore wagon used for heavy-haul traffic on Malmbanan consists of one car body and two three-piece bogies, each consisting of a bolster, two side frames and two wheelsets. The vehicle model in Fig. 1 has 14 DOFs. The unsprung mass of each wheelset is denoted  $M_w$ . Further,  $M_b$  and  $J_b$  are the mass and pitch moment of inertia for two side frames, while  $M_c$  and  $J_c$  are the mass and pitch moment of inertia for the car body (including bolsters). The axle distance within a bogie is  $\Delta_w$ , while the bogie centre distance is  $\Delta_b$ . Further, the vehicle model includes Hertzian wheel–rail contact stiffness, primary suspension stiffness  $k_1$  and damping  $c_1$ , and secondary suspension stiffness  $k_2$  and damping  $c_2$ . The sliding friction between bolster and side frames is modelled by a simplified Coulomb friction model using a tanh function (instead of the sign function) with friction coefficient  $\mu$  and normal load  $N$  [6]. Two of the vehicle DOFs represent the motion (vertical displacement and pitch rotation) of the car body, four DOFs represent the displacements and rotations of the two side frames, four DOFs the vertical displacement of the four wheels, while the four remaining DOFs are interfacing the track and are used in the formulation of the constraint equations [7]. For traffic on tangent track, it is

<sup>2</sup> Replace  $B$  with  $k$  or  $c$  depending on if it is a spring or a damper and let the spring/damper connect layers C and D.

assumed that the car body and bolster are rigidly connected. The axle load of current iron ore wagons is 32.5 tonnes, while the speed of loaded trains is 60 km/h. The parameter values for the vehicle model presented in Table 3 were collected from [5].

**Table 3.** Parameter values for vehicle model with axle load 32.5 tonnes

$M_c = 121 \times 10^3 \text{ kg}$	$J_c = 1.85 \times 106 \text{ kg.m}^2$	$M_b = 800 \text{ kg}$	$J_b = 730 \text{ kg m}^2$
$M_w = 1341 \text{ kg}$	$J_w = 100 \text{ kg m}^2$	$\Delta_w = 1.78\text{m}$	$\Delta_b = 6.77 \text{ m}$
$k_1 = 30 \text{ MN/m}$	$c_1 = 70 \text{ kNs/m}$	$k_2 = 3.75 \text{ MN/m}$	$c_2 = 10 \text{ kNs/m}$
	$\mu = 0.25$		

### 3 Iterative Approach for Prediction of Long-Term Differential Settlement

The simulation procedure is based on an iterative approach where the time-domain model of vertical dynamic vehicle–track interaction in the short-term is integrated with a model of ballast settlement in the long-term. In each iteration step, one time-domain simulation of short-term vehicle–track dynamics is performed. The calculated load maxima at the interface between each sleeper and ballast in the ballasted track section, generated by the combination of gravity load and each of the wheels of the vehicle model, are identified and used as input to an empirical settlement model. For each iteration step (in the short-term), the short-term model of the track dynamics is updated to account for the new states of the sleepers and ballast conditions, and it is assumed that the same set of load maxima is generated by all passing vehicles. By taking several iteration steps, the accumulated differential settlement in the long-term and the redistribution of foundation loads between adjacent sleepers are calculated [8]. In this work, an empirical settlement model inspired by a visco-plastic material mechanics model has been implemented by extending a model suggested by Sato [9]. For each vehicle model passage in iteration step  $j$  ( $j = 1, 2, \dots n_s$ ), the settlement  $\delta_{i,j}$  [m] below sleeper  $i$  ( $i = 1, 2, \dots N$ ) is formulated as a function of the maxima of sleeper–ballast contact force  $F_{s/b,i}$ :

$$\delta_{i,j} = \sum_{n=1}^{N_w} \left\{ \sum_{k=1}^{N_k} \alpha'_k \left[ \frac{\langle \max(F_{s/b,i})_n - F_{th,i} \rangle}{F_0} \right]^{\beta_k} \right\} \tag{1}$$

Here  $N_w$  is the number of wheels in the vehicle model, the parameters  $\alpha'_k$  and  $\beta_k$  are empirical, while  $F_0$  is a reference contact force with a unit such that the term within the square brackets becomes non-dimensional. This model assumes there is no accumulation of permanent ballast/subgrade deformation if the maximum sleeper–ballast contact pressure generated by a passing wheel is below a certain threshold value  $F_{th,i}$ . This is reflected in Eq. (1) using Macauley brackets  $\langle \cdot \rangle = 1/2(\cdot + |\cdot|)$ . Furthermore, it is assumed that the model provides the permanent deformation accounting for all the

layers of the substructure. The accumulated settlement at sleeper  $i$  after  $n_s$  iteration steps (corresponding to  $N_s$  load cycles) is calculated by summing the settlements calculated for each preceding step  $j$  as:

$$\Delta_i(n_s) = \sum_{j=1}^{n_s} \delta_{i,j} \tag{2}$$

For each sleeper  $i$ , it is assumed that the current threshold value  $F_{th,i}$  is dependent on the accumulated settlement  $\Delta_i$  as:

$$F_{th,i}(\Delta_i) = F_{th,\infty} - (F_{th,\infty} - F_{th,0})e^{-\gamma\Delta_i} \tag{3}$$

where  $F_{th,0}$  is the initial threshold value before traffic loading,  $F_{th,\infty}$  is the maximum threshold value that can be reached and  $\gamma$  is a parameter that determines the rate of hardening. In future work, these parameters need to be calibrated against field measurements. This approach leads to a nonlinear hardening (increase) of the threshold value with increasing settlement, see Fig. 2(a). In each iteration step, up to  $10^5$  load cycles (corresponding to 2 MGT of traffic) are considered. However, an adaptive step length is applied such that the maximum allowed settlement increment per iteration step is limited to 0.2 mm. If the increment exceeds 0.2 mm, a linear interpolation is applied.

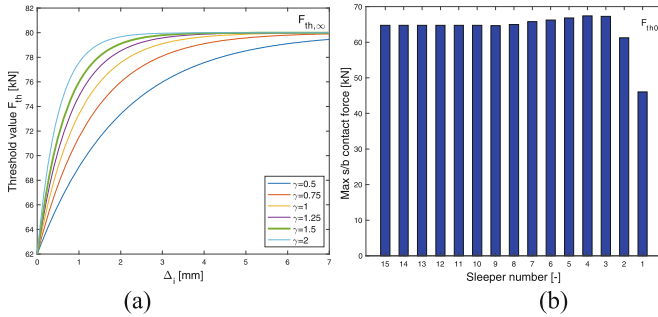


**Fig. 2.** (a) Influence of hardening parameter  $\gamma$  and accumulated settlement  $\Delta_i$  on threshold value  $F_{th}$  (here:  $F_{th,0} = 62$  kN and  $F_{th,\infty} = 80$  kN), (b) example of sleeper–ballast contact forces in the transition zone, where sleepers are numbered from the transition

## 4 Numerical Example

The simulation procedure is demonstrated by calculating the track settlement adjacent to a transition between ballasted track and 3 MB slab track due to an accumulated traffic load of 50 MGT. Note that any specific design of the track superstructure to smoothen the gradient in track stiffness at rail level has been disregarded in this example. To represent the early consolidation of the ballast, a uniform initial misalignment in vertical level between the different track forms has been assumed by prescribing a uniform initial offset  $\Delta_{\text{init}}$  of the ballast surface below each sleeper. Here  $\Delta_{\text{init}}$  is taken as 2 mm. The resulting irregularity in longitudinal level induces a pitching motion of the vehicle at the transition and an increased dynamic loading of the track. In addition, the change of track forms at the transition leads to a gradient in track stiffness at rail level. This leads to a further contribution to the transient excitation of the vehicle-track system and the differential settlement evolving in the ballasted track section.

For the evaluation of the settlement increment in each iteration step, it has here been assumed that  $\delta_{i,j}$  is calculated using a linear settlement equation ( $N_k = 1$ ,  $\beta_1 = 1$ ) with input data  $\alpha'_1 = 0.03$  mm per  $10^5$  load cycles,  $F_{\text{th},0} = 62$  kN,  $F_{\text{th},\infty} = 80$  kN,  $F_0 = 1$  kN and  $\gamma = 1.5$  1/mm.

The influence of axle load on the calculated time history of the vertical wheel-rail contact force at the transition is illustrated in Fig. 3(a). It is shown that the contribution to the dynamic load due to the stiffness gradient is smaller than the contribution due to the track irregularity. Further, the sleeper-ballast contact forces along the ballasted track have been calculated, see Figs. 2(b) and 3(b). In Fig. 2(b), it can be seen that the sleeper-ballast contact force for sleepers close to the transition (sleepers 3 to 5 from the transition) are higher than at other locations and exceeds the initial threshold value. As expected, the sleeper-ballast contact force increases with increasing axle load. Since it is assumed that the settlement increment is determined by the maximum sleeper-ballast contact force, see Eqs. (1)–(3), it can be concluded that the dynamic loading will lead to differential settlement, and consequently to an irregularity in longitudinal level, along the transition.

The calculated rail displacement after 50 MGT when only accounting for the gravity load is presented in Fig. 4. It can be seen that the uniform settlement ahead of the transition and the track irregularity (unloaded rail displacement) at the transition increase with increasing axle load.

In Fig. 5(a), the influence of train speed on the calculated time history of the vertical wheel-rail contact force at the transition is illustrated. As can be seen, the contribution to the dynamic load due to the stiffness gradient remains small in comparison to the contribution due to the track irregularity. Further, the sleeper-ballast contact force for sleepers near the transition (sleepers 3 to 5 from the transition) is higher than at other locations and exceeds the initial threshold value, see Fig. 5(b). For this application, it is observed that the influence of increasing train speed on sleeper-ballast force is negligible. For three different train speeds, the calculated rail displacement after 50 MGT when only accounting for the gravity load (unloaded rail displacement) is shown in Fig. 6. The influence of increasing train speed on the accumulated settlement is negligible.

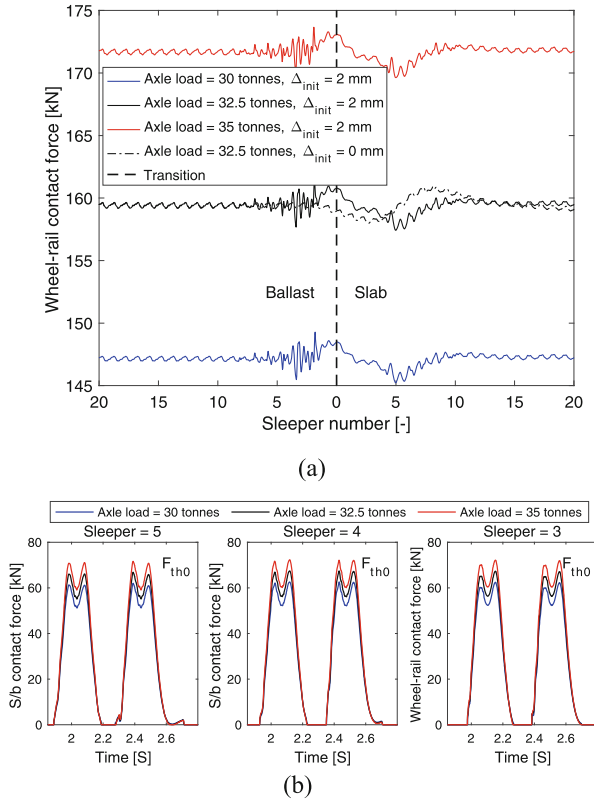


**Fig. 3.** Influence of axle load on (a) wheel–rail contact force for the leading wheelset, with uniform initial settlement  $\Delta_{init} = 0$  or 2 mm on the ballasted track, and (b) sleeper–ballast contact force for sleepers 3, 4 and 5. Results from the first iteration of the simulation procedure

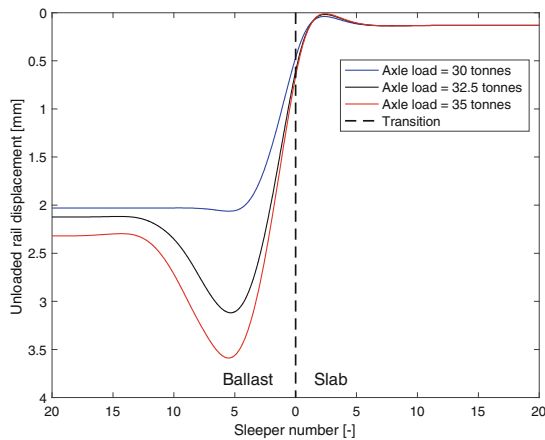


**Fig. 4.** Influence of axle load on rail displacement due to gravity load after an accumulated traffic load of 50 MGT. Train speed 60 km/h. Results for  $\Delta_{init} = 2$  mm

### 5 Conclusions

An iterative procedure to predict long-term degradation of longitudinal level due to accumulated settlement of ballasted track in a transition zone has been presented. It has been shown that differential settlement of sleepers near the transition is higher than elsewhere because sleeper–ballast contact forces are higher and exceed the prescribed threshold value in the settlement model. The stiffness gradient at the transition leads to a minor contribution to the dynamic load, while the influence of the irregularity is more significant. In a demonstration example, it was observed that the uniform settlement ahead of the transition and the track irregularity (unloaded rail displacement) at the transition increased with increasing axle load, but the influence of increasing train speed on the accumulated settlement was negligible. For future work, the model needs to be calibrated versus field measurements.

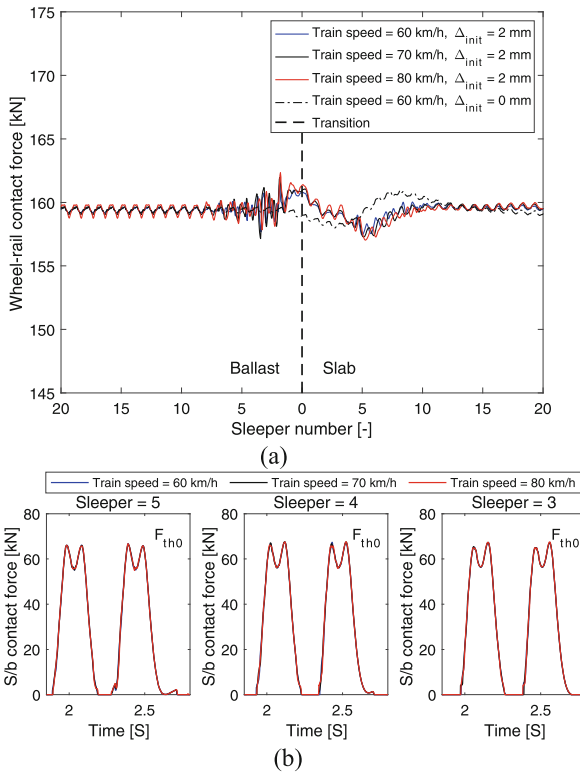


**Fig. 5.** Influence of train speed on (a) wheel–rail contact force for the leading wheelset, with uniform initial settlement  $\Delta_{init} = 0$  or 2 mm on the ballasted track, and (b) sleeper–ballast contact force for sleepers 3, 4 and 5. Results from the first iteration of the simulation procedure

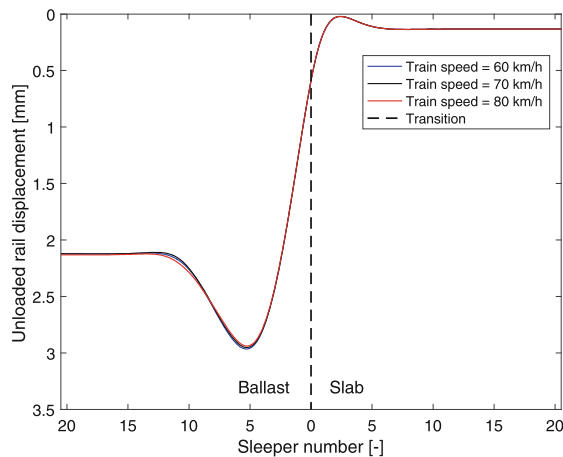


**Fig. 6.** Influence of train speed on unloaded rail displacement after an accumulated traffic load of 50 MGT. Axle load 32.5 tonnes. Results for  $\Delta_{\text{init}} = 2$  mm

**Acknowledgment.** The current study is part of the ongoing activities in CHARMEC—Chalmers Railway Mechanics ([www.chalmers.se/charmec](http://www.chalmers.se/charmec)). Parts of the study have been funded from the European Union’s Horizon 2020 research and innovation programme in the projects In2Track2 and In2Track3 under grant agreements Nos 826255 and 101012456. Discussions with Dr Saeed Hossein Nia, Mr Ingemar Persson and Mr Carlos Hermosilla are acknowledged. Parts of the simulations were performed using resources at Chalmers Centre for Componential Science and Engineering (C3SE) provided by the Swedish National Infrastructures for Computing (SNIC).

## References

1. Sañudo, R., Dell’Olio, L., Casado, J.A., Carrascal, I.A., Diego, S.: Track transitions in railways: a review. *Constr. Build. Mater.* **112**, 140–157 (2016)
2. Aggestam, E., Nielsen, J.C.O.: Multi-objective optimisation of transition zones between slab track and ballasted track using a genetic algorithm. *J. Sound Vib.* **446**, 91–112 (2019)
3. Morales-Gamiz, F.J.: Design Requirements, Concepts and Prototype Test Results for New System of Ballast Less System (3MB slab track) (2017)
4. Abadi, T., Le Pen, L., Zervos, A., Powrie, W.: A review and evaluation of ballast settlement models using results from the Southampton Railway Testing Facility (SRTF). *Proc. Eng.* **143**, 999–1006 (2016)
5. Nia, S.H.: On heavy-haul wheel damages using vehicle dynamics simulation. PhD thesis, Department of Aeronautical and Vehicle Engineering, KTH, Stockholm, Sweden (2017)
6. Andersson, S., Söderberg, A., Björklund, S.: Friction models for sliding dry, boundary and mixed lubricated contacts. *Tribol. Int.* **40**(4), 580–587 (2007)
7. Nielsen, J., Igeland, A.: Vertical dynamic interaction between train and track—influence of wheel and track imperfections. *J. Sound Vib.* **187**, 825–839 (1995)

8. Nielsen, J.C.O., Li, X.: Railway track geometry degradation due to differential settlement of ballast/subgrade—numerical prediction by an iterative procedure. *J. Sound Vib.* **412**, 441–456 (2018)
9. Sato, Y.: Optimization of track maintenance work on ballasted track. In: *Proceedings of the World Congress on Railway Research (WCRR '97)*, Florence, Italy, 16–19 November 1997, vol. B, pp. 405–411 (1997)